H. Nishikawa, M. Rad, and P.L. Roe , Grids and Solutions from Residual Minimisation,
Computational Fluid Dynamics 2000: Proceedings of the First International Conference on Computational Fluid Dynamics, ICCFD, Kyoto, Japan, 10-14 July 2000, Springer, 2001.

Grids and Solutions from Residual Minimisation

Hiroaki Nishikawa, Mani Rad, and Philip Roe

Department of Aerospace Engineering,
University of Michigan, Ann Arbor, MI 48109, USA

Abstract. In this paper, a least-squares method that incorporates node movement is presented. For nonlinear hyperbolic problems with bilinear flux functions, a class of quadrature formulae for fluctuation computation is proposed which allows a stable structure of discrete shocks, yet preventing nonphysical shocks. Computational results for Burgers' equation are shown to demonstrate its sharp shock capturing ability.

1 Introduction

One way to construct solutions of partial differential equations on triangular grids is to minimise residuals in a suitable norm with respect to nodal positions as well as solution values. It has been shown that such a method is capable of producing exact solutions for linear hyperbolic equations, automatically adjusting the mesh into a characteristic configuration [1–4]. It is an advantage of the method that a shock can be captured with many fewer nodes than the usual curvature adaptation [5]. However, its extension to nonlinear problems is not yet well-developed because of the difficulty in forming a characteristic mesh at nonlinear shocks. In this paper, we propose a way to accomplish this, i.e. a way to capture exact nonlinear shocks.

2 Quadrature Formulae

We consider sets of two-dimensional conservation laws of the form

$$\partial_x \mathbf{F}(\mathbf{w}) + \partial_y \mathbf{G}(\mathbf{w}) = 0 \tag{1}$$

where $\mathbf{F}$, $\mathbf{G}$, $\mathbf{w} \in \mathcal{R}^m$ in which each component of the fluxes is a bilinear function of the components of $\mathbf{w}$.

$$\mathbf{F}(\mathbf{w}) = \mathbf{w}^t \mathbf{C} \mathbf{w}, \qquad \mathbf{G}(\mathbf{w}) = \mathbf{w}^t \mathbf{D} \mathbf{w} \tag{2}$$

where $\mathbf{C}$ and $\mathbf{D}$ are constant symmetric third-order tensors. This structure includes the Euler equations of compressible inviscid flow if $\mathbf{w}$ is taken to be Roe's parameter vector. We are interested in solving (1) by a least-squares method on triangular grids in which the first step is to compute the fluctuation.

$$\mathbf{\Phi}_{123} = \int\!\!\int_{123} [\partial_x \mathbf{F}(\mathbf{w}) + \partial_y \mathbf{G}(\mathbf{w})]\, dxdy = \oint_{123} [\mathbf{F}(\mathbf{w}) dy + \mathbf{G}(\mathbf{w}) dx] \tag{3}$$

where the data is available at the vertices 1,2,3. The second step is then to distribute some fraction of the fluctuation to each vertex. In this least-squares method, as will be explained in Section 5, these fractions sum to zero over any given element, so that the method will be conservative however the fluctuations are evaluated. Therefore we focus first on different properties of various evaluations. Consider a single term, arising from integrating just one component of the flux vector over on edge of the element.

$$\mathbf{F}_{12} = \int_1^2 \mathbf{F}(\mathbf{w})\ dy = \int_1^2 \mathbf{w}^t \mathbf{C} \mathbf{w}\ dy \tag{4}$$

To evaluate this integral there is a class of simple formulae;

$$\mathbf{F}_{12}(\alpha) = \frac{(y_2 - y_1)}{2} \left[(\mathbf{w}_1^t \mathbf{C} \mathbf{w}_2 + \mathbf{w}_2^t \mathbf{C} \mathbf{w}_1) + \alpha (\mathbf{w}_1 - \mathbf{w}_2) \mathbf{C} (\mathbf{w}_1 - \mathbf{w}_2) \right] \tag{5}$$

where α is a parameter that has only a second-order relative effect on the accuracy of the estimate as clearly seen.

3 Formulae for the Fluctuation

The formula for the fluctuation is obtained by summing up the contributions from three sides. Introducing the notation,

$$\mathbf{w}_{ij}(\alpha) = \frac{\alpha}{2}(\mathbf{w}_i + \mathbf{w}_j) + (1-\alpha)\mathbf{w}_k \tag{6}$$

where i, j, k are cyclically permuted for $1, 2, 3$, and rearranging terms, we obtain

$$\begin{aligned} \boldsymbol{\Phi}_{123}(\alpha) = \mathbf{w}_{31}^t(\alpha) \left\{ \Delta y_3 \mathbf{C} - \Delta x_3 \mathbf{D} \right\} (\mathbf{w}_3 - \mathbf{w}_1) + \\ \mathbf{w}_{12}^t(\alpha) \left\{ \Delta y_2 \mathbf{C} - \Delta x_2 \mathbf{D} \right\} (\mathbf{w}_2 - \mathbf{w}_1) \end{aligned} \tag{7}$$

where Δy_i is the difference of y taken anticlockwise along the edge opposite to the node i, similarly for Δx_i. Note that this formula is not symmetric with respect to the vertices. There are two other rearrangements possible, and all three will give the same numerical value. This particular arrangement can be written

$$\begin{aligned} \boldsymbol{\Phi}_{123}(\alpha) = \left\{ \frac{\partial \mathbf{F}}{\partial \mathbf{w}} \Delta y_3 - \frac{\partial \mathbf{G}}{\partial \mathbf{w}} \Delta x_3 \right\} (\mathbf{w}_3 - \mathbf{w}_1) + \\ \left\{ \frac{\partial \mathbf{F}}{\partial \mathbf{w}} \Delta y_2 - \frac{\partial \mathbf{G}}{\partial \mathbf{w}} \Delta x_2 \right\} (\mathbf{w}_2 - \mathbf{w}_1) \end{aligned} \tag{8}$$

where the Jacobian matrices in the first term are evaluated at the state $\mathbf{w}_{31}(\alpha)$ and those in the second terms at the state $\mathbf{w}_{12}(\alpha)$, which shows that the parameter α acts on the Jacobian matrices. For example, taking $\alpha = 2/3$ we obtain the so-called conservative linearisation which has been utilised in the fluctuation splitting method [6].

3.1 Shock Recognition: $\alpha = 1$

Suppose that two of the states happen to be equal, $\mathbf{w}_1 = \mathbf{w}_2 = \mathbf{w}_c$. Then the second line of (7) vanishes and the first line becomes

$$\boldsymbol{\Phi}_{123}(\alpha) = \mathbf{w}_{31}^t(\alpha)\left\{\Delta y_3\mathbf{C} - \Delta x_3\mathbf{D}\right\}(\mathbf{w}_3 - \mathbf{w}_c). \tag{9}$$

For the special choice $\alpha = 1$, which gives $\mathbf{w}_{31}(\alpha) = \overline{\mathbf{w}}_{31} = (\mathbf{w}_3 + \mathbf{w}_c)/2$, this corresponds precisely with the Hugoniot condition,

$$\overline{\mathbf{w}}^t(S\mathbf{C} - \mathbf{D})\Delta\mathbf{w} = 0 \tag{10}$$

along the edge 31, provided the edge 12 is aligned in shock of the speed $dy/dx = S$. Note that this is independent of the position of the other node. However, unfortunately, this admits nonphysical shocks as well.

3.2 Special Properties: $\alpha = 0$

For scalar problems, the choice $\alpha = 0$ has a special property. With $\alpha = 0$, the fluctuation becomes

$$\begin{aligned}\boldsymbol{\Phi}_{123}(0) = \mathbf{w}_2^t\left\{\Delta y_3\mathbf{C} - \Delta x_3\mathbf{D}\right\}(\mathbf{w}_3 - \mathbf{w}_1) +& \\ \mathbf{w}_3^t\left\{\Delta y_2\mathbf{C} - \Delta x_2\mathbf{D}\right\}(\mathbf{w}_2 - \mathbf{w}_1)&\end{aligned} \tag{11}$$

where all quantities are thought of as scalar. Now suppose the edge 12 is aligned with the characteristic whose speed evaluated at the state 2, i.e. *on the edge itself*. Then the first term vanishes. And the second approximates the characteristic equation $d\mathbf{w} = 0$ exactly, again for any position of the third node.

Another important property associated with this choice is the ability to compute physical rarefaction. To see this, consider Burgers' equation $\partial_t u + \partial_x f = 0$ where $f = u^2/2$. Discretising the spatial derivative term by the quadrature formula (5), rearranging the terms, we find

$$\partial_t u_j + \frac{f_{j+1} - f_{j-1}}{2\Delta x} = (1-\alpha)\Delta x^2 \frac{u_{j+1} - u_{j-1}}{2\Delta x}\frac{u_{j+1} - 2u_j + u_{j-1}}{\Delta x^2} \tag{12}$$

which is a second order discretisation of

$$\partial_t u + \partial_x f = (1-\alpha)\Delta x^2\, \partial_x u\; \partial_x^2 u. \tag{13}$$

This shows that for diverging characteristics, $\partial_x u > 0$, taking $\alpha < 1$ gives positive dissipation. Experimentally we find that α needs to be well below unity, and that zero is a good choice.

4 Detecting Compression/Expansion

One possible way to take advantage of the formulae for the fluctuation is to use $\alpha = 1$ for elements in shocks and $\alpha = 0$ for others, thus capturing shocks exactly at the same time avoiding possible rarefaction shocks. The decision can be made based on the rate of change of the triangle area due to the virtual vertex motion caused by the characteristic speeds. Imagine that a triangle is convected in a characteristic field. If the characteristics are diverging, implying expansion, the triangle area would increase. On the other hand, if the characteristics are converging, implying compression, the triangle area would decrease. It is easy to show that the rate of change of the area is given by

$$\frac{dS_T}{dt} = \frac{1}{2} \sum_{i=1,2,3} \boldsymbol{\lambda}_i \cdot \mathbf{n}_i \tag{14}$$

where $\mathbf{n}_i$ is the scaled inward normal vector opposite to the vertex i, and $\boldsymbol{\lambda}_i$ is a characteristic speed vector at vertex i. For system of equations, we compute this for each wave-like component.

5 Least-Squares Formulation

The solutions are sought that minimise the norm

$$\mathcal{F} = \sum_{T \in \{T\}} F_T = \frac{1}{2} \sum_{T \in \{T\}} \frac{\boldsymbol{\Phi}_T^t Q_T \boldsymbol{\Phi}_T}{S_T} \tag{15}$$

over a set $\{T\}$ of triangular elements that divides the domain of interest. Q_T is a positive definite symmetric matrix that assigns relative weight to the different equations [1]. The change made to each vertex $\{j\}$ is the sum of the contribution from the surrounding triangles $\{T_j\}$, and can be written in the fluctuation splitting format as follows.

$$\delta \mathbf{w}_j = -\omega_u \sum_{T \in \{T_j\}} \mathcal{A}_j^T \boldsymbol{\Phi}_T \tag{16}$$

$$\delta \mathbf{x}_j = -\omega_x \sum_{T \in \{T_j\}} \left\{ \mathcal{B}_j^T \boldsymbol{\Phi}_T - \frac{F_T}{2S_T} \mathbf{n}_j \right\} \tag{17}$$

where $\mathbf{w}_j$ is a solution vector at the node, $\mathbf{x}_j$ is the nodal position vector, and ω_u and ω_x are small constants. The second term in (17) comes from differentiating the weight $1/S_T$ in the norm. Note that the scheme is equivalent to the steepest descent method. $\mathcal{A}_j^T$ and $\mathcal{B}_j^T$ are the distribution matrices given by

$$\mathcal{A}_j^T = \frac{1}{S_T} \left(Q_T \frac{\partial \boldsymbol{\Phi}_T}{\partial \mathbf{w}_j} \right)^t \tag{18}$$

$$\mathcal{B}_j^T = \frac{1}{S_T} \left(Q_T \frac{\partial \boldsymbol{\Phi}_T}{\partial \mathbf{x}_j} \right)^t . \tag{19}$$

Here the computation of the derivative in $\mathcal{A}_j^T$ requires careful consideration. We have observed that taking the derivative straightforwardly can result in completely wrong solutions. As suggested in [7], it is important to linearise the equations first and then apply the least-squares method. This means that we take the derivatives assuming $\mathbf{w}_{ij}(\alpha)$ are constant in (7) because these quantities act on the Jacobian matrix as mentioned before. Yet this raises another important point of consideration. Recall that the fluctuation has two other rearrangements other than (7). The derivative computed as above now depends on this arrangement. Then it would be reasonable to take the arithmetic average of the three possible forms and take the derivative, which yields

$$\frac{\partial \mathbf{\Phi}_T}{\partial \mathbf{w}_1} = \frac{\mathbf{w}_{31}^T(\alpha)}{3}\left[(\Delta y_1 - \Delta y_3)\mathbf{C} - (\Delta x_1 - \Delta x_3)\mathbf{D}\right] + \frac{\mathbf{w}_{12}^T(\alpha)}{3}\left[(\Delta y_1 - \Delta y_2)\mathbf{C} - (\Delta x_1 - \Delta x_2)\mathbf{D}\right]. \tag{20}$$

6 Results

Preliminary results are available for Burgers' equation $\partial_y u + u\ \partial_x u = 0$, for which Q_T was taken to be unity. Figures 1 and 2 show the final grid and solution for a right-moving curved shock for the boundary conditions; $u = 3$ for $x \leq -0.8$ and $\frac{30}{17}(x-1)$ for $x \geq -0.7$ where the data is interpolated linearly between $x = -0.8$ and $x = -0.7$, modeling an initial discontinuity. The grid and the solution were obtained by repeating the following cycle.

1. Converge the solution on a fixed grid
2. Assign α to each element, depending the sign of (14)
3. Remove undesirable nodes
4. Update solutions and coordinates, with edge swappings interleaved (2000 iterations maximum)

and the method terminates when the changes to solutions and coordinates are both small in the step 4 or the maximum number of cycles is reached, say 20. The edge swapping is based on the norm reduction, which attempts to create a characteristic mesh as clearly seen in the results. Also, because two edges sometimes try to represent the same characteristic we implemented a scheme for removing redundant nodes. The method converged at 10 cycles. And the final values of α are 1 for the elements forming a shock, and 0 elsewhere.

A grid aligned expansion wave was computed with $u = -0.8$ on the left and $u = 0.8$ on the right, to demonstrate the ability of the method to compute entropy-satisfying solutions. The values of α are automatically set to be zero everywhere in the step 2, and as can be seen the final solution is the correct smooth expansion fan. The method converges at just 1 cycle. Increasing the value of α, we found that a rarefaction shock appeared in the middle of the rarefaction and it became finally a perfectly-resolved rarefaction shock when $\alpha = 1$. This is consistent with the observation in section 3.2.

7 Conclusions

A least-squares method that incorporates node movement and a class of integration rules has been presented. The preliminary results demonstrated its ability

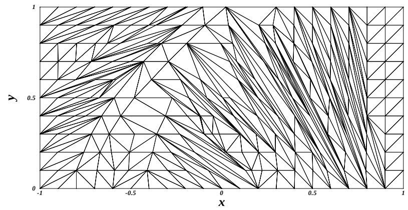

Fig. 1. The final grid for the curved shock.

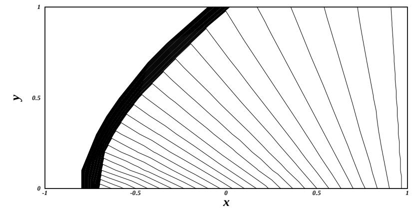

Fig. 2. Solution contours for the shock.

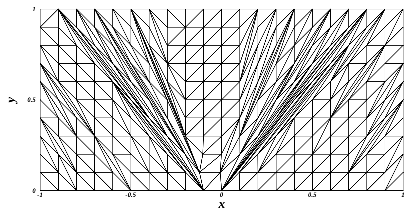

Fig. 3. The final grid for the expansion.

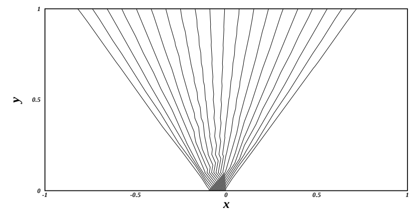

Fig. 4. Solution contours for the expansion.

to compute shocks extremely sharply as well as to avoid nonphysical shocks. In future work we will focus on improving the efficiency of the method, especially the mechanism for removing redundant nodes, and on the extension to systems of equations. In this latter task we expect the proper choice of Q_T in (15), which defines the minimization norm, to be important.

References

1. P. L. Roe: 'Compounded of Many Simples'. In: *Barriers and Challenges in Computational Fluid Dynamics*, ed. by V. Venkatakrishnan, M. D. Salas, Sukumar R. Chakravarthy (Kluwer Academic Publishers 1998) pp. 241-158
2. P. L. Roe: 'Fluctuation Splitting Scheme on Optimal Grids'. In: *AIAA 13th CFD Conference*, June 1997, Paper 97-2034
3. M. J. Baines, S. J. Leary, M. E. Hubbard: 'A Finite Volume Method for Steady Hyperbolic Equations'. In: *Finite Volumes for Complex Applications II, problems and perspectives, 2nd International Symposium at Duisburg, Germany, July 19–22, 1999*, ed. by R. Vilsmeier, F. Benkhaldoun, D. Hanel (Hermes Science Publications, Paris 1999) pp. 787–794
4. W. A. Wood, W. L. Kleb: 'On Multi-dimensional Unstructured Mesh Adaptation'. In: *AIAA 14th CFD Conference*, June 1999, Paper 99-3254
5. W. G. Habashi, J. Dompierre, Y. Bourgault, D. Ait-Ali-Yahia, M. Fortin, M. Vallet: In: Int. J. for Num. Meth. Fluids **32**, 725-744 (2000)
6. H. Deconinck, P. L. Roe, R. J. Struijs: In: Computers and Fluids **22**, No. 2/3, 215-222, (1993)
7. B. Jiang: *The Least-Squares Finite Element Method: Theory and Applications in Computational Fluid Dynamics and Electromagnetics* (Springer-Verlag New York 1998)